TMA4212: Project 2

Anne Asklund, Paulius Cebatarauskas, Jasper Steinberg

3rd June 2022

1 Introduction

In this project we investigate different numerical schemes. First we look at heat distribution on the unit square for non-perpendicular heat flow directions, with both an equidistant grid and a non-equidistant grid. We then consider heat distribution of the first quadrant of the unit disk with different methods for the boundary approximation. Finally, we look at a transport equation with variable coefficients, considering both an upwind and a Lax-Wendroff scheme.

2 Heat distribution in anisotropic materials

$$-\mathcal{L}_h u = -\nabla \cdot (\kappa \nabla u) = f \quad \text{in} \quad \Omega \tag{1}$$

is a model which applies to the stationary heat flux in anisotropic materials with heat conductivity κ, internal heat sources f, and conservation of energy. We consider a 2-dimensional domain with heat flow in directions

$$\vec{d_1} = (1, 0) \quad \text{and} \quad \vec{d_2} = (1, r) \quad \text{for} \quad r \in \mathbb{R}.$$

This gives κ the form, where $a > 0$,

$$\kappa = \begin{pmatrix} 1+a & r \\ r & r^2 \end{pmatrix}.$$

Rewriting (1) with directions $\vec{d_1}$ and $\vec{d_2}$ in mind,

$$f = -\nabla \cdot (\kappa \nabla u) = -(a+1)\partial_x^2 u - 2r\partial_x \partial_y u - r^2 \partial_y^2 u = -a\partial_x^2 u - (\vec{d_2} \cdot \nabla)^2 u. \tag{2}$$

2.1 An equidistant grid on the unit square

Suppose $r = 1$. Then we can consider (2) on the domain $\Omega = [0, 1]^2$ with Dirichlet boundary conditions $u = g$ on $\partial\Omega$ as a uniformly spaced grid. We discretize with M steps in both the x and y direction such that $x_m = hm$ and $y_n = hn$ where $h = \frac{1}{M}$ such that there are $M + 1$ steps in each direction. Using second order differences in directions $\vec{d_1}$ and $\vec{d_2}$

$$\delta_x^2 U = \frac{U_{m+1,n} - 2U_{m,n} + U_{m-1,n}}{h^2}.$$

and

$$\left[(\vec{d_2} \cdot \nabla)^2\right]_h U = \frac{U_{m+1,n+1} - 2U_{m,n} + U_{m-1,n-1}}{h^2}.$$

The derivative in $\vec{d_2}$-direction does not have an extra factor of $\|r\|^2$ in the denominator as we consider the vector $\vec{d_2}$ and not a derivative with respect to the unit vector $\hat{\vec{d_2}}$

With these finite differences the stencil for the numerical scheme becomes

$$2(1+a)U_{m,n} - a(U_{m+1,n} + U_{m-1,n}) - (U_{m+1,n+1} + U_{m-1,n-1}) = h^2 f. \tag{3}$$

In general a scheme is monotone if, when written in the form

$$\alpha_{m,n}U_{m,n} - \sum_{(l,l')\neq(0,0)}\sum \beta_{m+l,n+l'}U_{m+l,n+l'} + c_{m,n} = 0, \tag{4}$$

where $\alpha_{m,n} > 0$, $\beta_{m,n} \geq 0$, $c_{m,n} \in \mathbb{R}$, and $\alpha_{m,n} \geq \sum\sum \beta_{m+l,n+l'}$. Scheme (3) is monotone as

$$\alpha_{m,n} = 2(1+a) > 0, \quad \beta_{m+l,n+l'} = 1 \text{ or } a > 0, \quad \text{and} \quad \sum\sum \beta_{m+l,n+l'} = 2a + 2 = \alpha.$$

To show L^∞-stability of the scheme consider the comparison function $\phi(x,y) = \frac{1}{2}x(1-x)$ on our domain $[0,1]^2$. Then $\phi \geq 0$ and at any point P

$$-\mathcal{L}_h\phi_P = 1 + a > 1.$$

Consider V_P which solves (3) at point P and $V_P = 0$ on $\partial\Omega$. Define $W_P = V_P - \|f\|_\infty$. Then

$$-\mathcal{L}_h W_P = -\mathcal{L}_h V_P - \|f\|_\infty(-\mathcal{L}_h\phi_P) = f_P - (a+1)\|f\|_\infty \leq 0.$$

As $-\mathcal{L}_h$ is monotone and $-\mathcal{L}_h \leq 0$, by the discrete maximum principle (DMP)

$$W_P \leq \max_{\partial\Omega} W_P \leq 0 \implies V_P \leq \|f\|_\infty\phi_P.$$

Conversely, consider $W = -V_P - \|f\|_\infty\phi_P$ which satisfies

$$-\mathcal{L}_h W_P = -f_P - (a+1)\|f\|_\infty \leq 0.$$

Then by the DMP

$$W_P \leq \max_{\partial\Omega} W_P \leq 0 \implies -V_P \leq \|f\|_\infty\phi_P.$$

Thus

$$\max|V_P| \leq \|f\|_\infty \max\phi_P \tag{5}$$

and (3) is L^∞-stable with respect to a right-hand side.

Let the local truncation error of the scheme at point P be $\tau_P = \mathcal{L}_h u - \mathcal{L}u$. Then

$$\begin{aligned}
\tau_P &= (\frac{1}{h^2}\delta_x^2 - \partial_x^2)u + (\frac{1}{2h^2}\delta_{\vec{d_2}}^2 - (d_2\vec{\cdot}\nabla)^2)u \\
&= a\frac{1}{12}h^2 u_{xxxx}(\xi_m,\eta_n) + \frac{1}{12}(\sqrt{2}h)^2(\vec{d_2}\cdot\nabla)^4 u(\xi_m^{'},\eta_n^{'}) \\
&\leq \frac{1}{12}h^2 K \qquad \text{if} \qquad K = a\|u_{xxxx}\|_{L^\infty(\Omega)} + 2\|(\vec{d_2}\cdot\nabla)^4 u\|_{L^\infty(\Omega)}.
\end{aligned}$$

Let the error at point P be $e_P = u_P - U_P$. Then $-\mathcal{L}_h e_P = -\tau_P$ and as we have Dirichlet BCs $e_P = 0$ on $\partial\Omega$. Using the L^∞-stability and noting that $\max\phi_P = \frac{1}{8}$,

$$\|e\|_\infty \leq \frac{1}{96}Kh^2 \tag{6}$$

Thus, smooth solutions should converge with $O(h^2)$.

For two examples of scheme (3) applied in practice we consider the two functions $u_1(x,y) = y\sin(\pi x)$ and $u_2(x,y) = y^2\arctan(x)$ as exact solutions. Then the respective right hand sides become $f_1(x,y) = 2a+4$ and $f_2(x,y) = \frac{2y}{x^2+1}\left(2 - (1+a)\frac{xy}{x^2+1} + 2\arctan(x)\right)$. Figure 1 shows the numerical solutions to these problems with corresponding log-log plots of the errors. We see that for both examples we have achieved second order convergence.

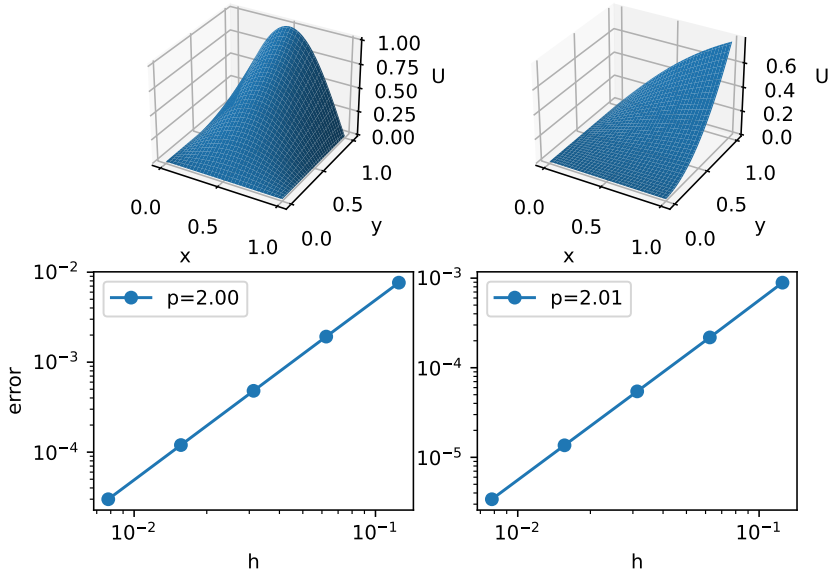

Figure 1: Figure showing numerical solution and convergence of errors for u_1 and u_2 for the regular grid.

2.2 An irregular grid on the unit square

Now consider an irregular grid such that r is irrational and $k = |r|h$. Note that the scheme itself does not change as it is independent of r. However, as r is irrational, our grid will now miss the upper boundary as there is no integer such that $N = \frac{M}{|r|}$. For this reason, we thus choose to "fatten the boundary", and set $U_{m,N+1} = g(P)$ where P is the point on the boundary closest to $U_{m,N+1}$. This method is of order k and so our method is now of order $O(h^2 + k) = O(k)$.

To illustrate, let $r = \sqrt{2}$ and let $N = \left\lceil \frac{M}{|r|} \right\rceil$ such that there are $N + 1$ intervals in the y-direction.

Figure 2 shows the solution u_1 and linear convergence of the maximum error for the first example in the previous section. We see that the error now has linear convergence.

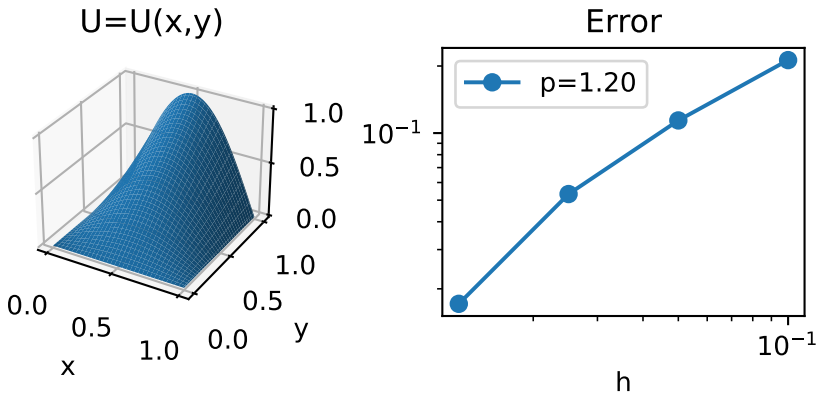

Figure 2: Figure showing numerical solution and convergence of errors for u_1 for the irregular grid.

2.3 A grid on the first quadrant

We let Ω denote the part of the unit disc that is in the first quadrant. The boundary then consists of the three following curves

$$\gamma_1 = [0,1] \times \{y = 0\}, \quad \gamma_2 = \{x = 0\} \times [0,1], \quad \gamma_3 = \{(x, \sqrt{1-x^2}) \mid x \in [0,1]\}.$$

We will solve (1) for the case when $\kappa = I$ is the identity matrix. Then our problem becomes

$$-\nabla \cdot (\kappa \nabla u) = -\Delta u = h \qquad \text{in} \qquad \Omega,$$

where h is a known function. Let $h = \frac{1}{M}$ where M is some positive natural number. We will use a equidistant grid on the unit square, defined as $\{(ih, jh) : i, j = 0, \ldots, M\}$. For points $U_{m,n}$, whose neighbouring points are also inside our grid, we use second order differences to approximate $\partial_x^2, \partial_y^2$ which yield the following scheme:

$$\Delta u(x_m, t_n) = \frac{1}{h^2}\delta_x^2 u_{m,n} + \frac{1}{h^2}\delta_y^2 u_{m,n} + O(h^2) = \frac{u_{m+1,n} + u_{m-1,n} - 4u_{m,n} + u_{m,n+1} + u_{m,n-1}}{h^2} + O(h^2)$$

But for points $U_{m,n}$ whose neighbouring points are outside γ_3, we have to adjust our scheme. We solve this issue using two different methods. The first method is to fatten the boundary. We approximate points outside the boundary by setting them equal to the value at the normal projection onto γ_3, and leave our scheme unchanged. This resembles how we usually treat points that happen to be on the boundary.

The second method is to modify the discretisation close to the boundary. Assume that we want to apply a difference approximation for ∂_x^2 to the point U_P. This means that we need the points U_W, and U_E, where W stands for west and E stands for east. Assume that U_E lies outside our boundary. Then we introduce $U_{E'}$ such that $E' = P + (\eta_1 h, 0)$. We then wish to find coefficient $a_W, a_{E'}, a_P$ such that

$$\partial_x^2 U_P = a_W U_W + a_P U_P + a_{E'} U_{E'} + \tau_{x,h},$$

where $\tau_{x,h}$ is the truncation error. Using the method of undetermined coefficients we find that

$$a_{E'} = \frac{2}{h^2(\eta_1^2 + \eta_1)}, \quad a_W = \frac{2}{h^2(1+\eta_1)}, \quad a_P = -\frac{2}{h^2\eta_1}.$$

Now we apply the same method to find an approximation for ∂_y^2 to the point U_P. We need the points U_S, and U_N, where S stands for south and N stands for north. Assume that U_N lies outside our boundary. Then we introduce $U_{N'}$ such that $N' = P + (0, \eta_2 h)$. We then wish to find coefficient $a_S, a_{N'}, a_P$ such that

$$\partial_x^2 U_P = a_S U_S + a_P U_P + a_{N'} U_{N'} + \tau_{y,h},$$

where $\tau_{y,h}$ is the truncation error. Using the method of undetermined coefficients we find that

$$a_{N'} = \frac{2}{h^2(\eta_2^2 + \eta_2)}, \quad a_S = \frac{2}{h^2(1+\eta_2)}, \quad a_P = -\frac{2}{h^2\eta_2}.$$

It was easier to implement the fattening of the boundary. This should be quite clear, just from the explanation of the two methods. For the second method we needed to change our scheme for points near the boundary γ_3. This led to quite a lot of code which was hard to write, and hard to read. Even though the code was hard to program and to understand, it executed faster. We timed both codes, where we used M=40. The code which implemented fattening the boundary used $0.22s$ on average. Using the second method, where we modified our scheme, yielded a code which ran in $0.18s$. Even though it was faster, the difference is so small that I would rather use the simpler to implement method of fattening the boundary. Although, if you needed a very fine grid, it could become quite more practical to modify our scheme near the boundary.

In figure (3) we have used the fattening boundary method, with $M = 5$. The exact solution we tried to model was $u(x, y) = e^{-(x^2+y^2)}$. The plot on the left side seems to correspond to that solution quite nicely, even for small values of M. For the plot on the right side, we have computed

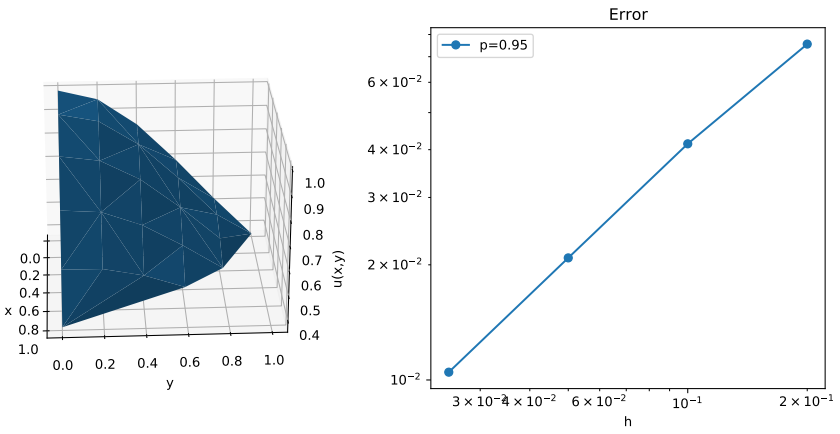

Figure 3: Figure showing numerical solution and convergence of error for fattening the boundary.

the error of our approximated solution compared to our exact solution. This method seems to have order one of convergence as expected. Our approximation in the interior of our domain is of second order, but our difference approximation near the boundary is only first order, as the plot shows.

In figure (4) we have used the method of modifying the discretisation near the boundary, with $M = 5$. The exact solution we tried to model was $u(x, y) = x^2 + y^2$. The plot on the left side corresponds to that solution quite nicely, even for small values of M. For the plot on the right side, we have computed the error of our approximated solution compared to our exact solution. This method has order one of convergence, since we lose one order when modifying the discretisation. This is due to the lack of cancellation of terms, when we use Taylor expansions. Our approximation in the interior of our domain is the same as in the previous method, but our difference approximation near the boundary is only first order, as the plot shows.

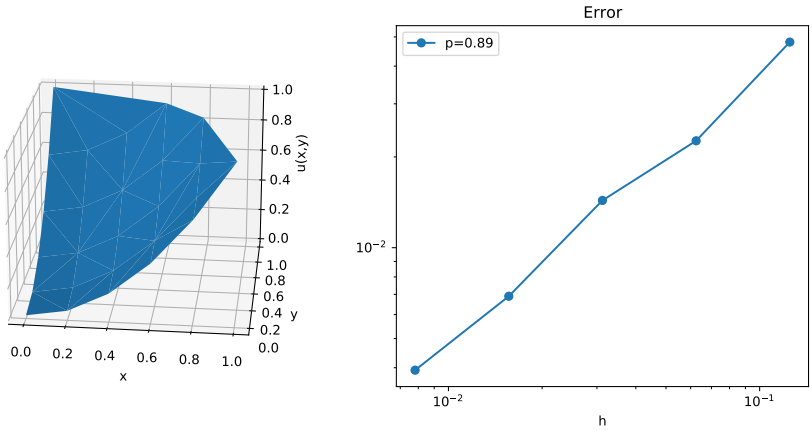

Figure 4: Figure showing numerical solution and convergence of error for modifying discretisation.

3 A variable coefficient transport equation

We consider the problem

$$\begin{cases} u_t + a(x,t)u_x = 0 & \text{in} \quad (0,1) \times (0,T), \\ u(x,0) = u_0(x) & \text{in} \quad [0,1], \\ u(0,t) = g(t) & \text{in} \quad [0,T]. \end{cases} \tag{7}$$

For this problem to be well-posed we need that a is nice enough, that is,

$$a \in C^1([0,1] \times [0,T]), \quad a(0,t) > 0, \quad \text{and} \quad a(1,t) > 0. \tag{8}$$

For interior nodes the upwind scheme is

$$U_m^{n+1} = (1 - r^+ - r^-)U_m^n + r^+ U_{m-1}^n + r^- U_{m+1}^n \quad \text{such that} \quad r^\pm = \frac{k}{h} a^\pm,$$

where $a^+ = \max\{a, 0\}$ and $a^- = \max\{-a, 0\}$. In addition, h, k are the stepsizes in x and y direction, respectively. Note that $|r| = r^+ + r^-$ and $r = r^+ - r^-$.

The upwind scheme is monotone if (4) is satisfied with its conditions, if we replace indices $\cdot_{m,n}$ with $\cdot_m^n$. In this scheme $c_m^n = 0$. The scheme gives us that $\alpha_m^{n+1} = 1 > 0$. $\beta_{m\pm1}^n = r^\pm \geq 0$. $\beta_m^n = 1 - r^+ - r^- = 1 - |r|$. We get that $1 - |r| \geq 0$ if and only if $|r| \leq 1$. This is our CFL-condition and if the CFL holds, then our scheme is monotone.

Von Neumann

Let $U_m^n = \xi^n e^{i\beta x_m}$, where i is such that $i^2 = -1$, and $\beta \in \mathbb{R}$. The scheme is von Neumann stable if $|\xi| \leq 1$. Applying this ansatz to our scheme and dividing by $\xi^n e^{i\beta x_m}$ yields

$$\xi = (1 - r^+ - r^-) + r^+ e^{-ih} + r^- e^{ih}$$

We split this up into three cases.

($r = 0$) In this case $\xi = 1$ and $|\xi| \leq 1$ trivially.

($r > 0$) This means that $r^- = 0$, so $\xi = (1 - r^+) + r^+ e^{-ih}$. This is a circle in the complex plane with center at $1 - r^+$ and radius r^+. Then $|\xi|$ is the distance between origin and the periphery of this circle. Thus $|\xi| \leq 1$ if $r^+ \leq 1$.

($r < 0$) This means that $r^+ = 0$, so $\xi = (1 - r^-) + r^- e^{ih}$. This is a circle in the complex plane with center at $1 - r^-$ and radius r^-. Then $|\xi|$ is the distance between origin and the periphery of this circle. Thus $|\xi| \leq 1$ if $r^- \leq 1$.

The constraints $r^\pm \leq 1$, means that $|r| \leq 1$, which is the CFL condition. If this condition holds, then our scheme is von Neumann stable.

Dissipative & Dispersive

Let $U_m^n = \rho^n e^{i(\omega t_n + \beta x_m)}$ where $\rho \geq 0$ and insert this into the scheme. Simplify the resulting scheme by dividing the equation by $\rho^n e^{i(\omega t_n + \beta x_m)}$, which yields

$$\rho e^{i\omega k} = (1 - |r|) + r^+ e^{-i\beta h} + r^- e^{i\beta h}$$

Applying Euler's formula, and collecting terms

$$= (1 - |r|) + |r| \cos(\beta h) + + ir \sin(\beta h).$$

Taking the norm on both sides yields

$$\rho^2 = Im^2 + Re^2 = 1 - |r|(1 - |r|)4 \sin^2\left(\frac{\beta h}{2}\right)$$

after use of of some trigonometric identities. Using that $\sin^2 \leq 1$, which yields that under the condition that $|r| \leq 1$ we have $\rho^2 \leq 1$. This means that our scheme is dissipative.

The scheme will be dispersive if $\frac{\omega}{\beta}$ is not constant. Thus, if ω is not a first order polynomial of β, then our scheme is dispersive. We get an expression for ω by computing the argument of $\rho e^{i\omega k}$, which yields

$$\omega k = \arg(\rho e^{i\omega k}) = \arctan\left(\frac{-r\sin(\beta h)}{1-|r|+|r|\cos(\beta h)}\right).$$

This is clearly not a first order polynomial of β, hence $\frac{\omega}{\beta}$ will be non-constant, and thus our scheme is dispersive.

The Upwind Scheme

For the upwind scheme we chose to implement it with $a(x) = \frac{1}{2} - e^{-5\left(x-\frac{1}{2}\right)^2}$, notice that $a(x)$ is is sign changing on $[0,1]$. We also decided to add a right-hand side, for simplified numerical testing. Our exact test solutions were $u_1(x,t) = \cos(2\pi x)\sin(t)$ and $u_2(x,t) = te^{-x}$. The respective right hand sides became $f_1(x,t) = \cos(t)\cos(2\pi x) - 2\pi a(x)\sin(t)\sin(2\pi x)$ and $f_2(x,t) = (1-ta(x))\,e^{-x}$. Figure 3 shows the numerical solution and log-log plots of the error in both space and time for u_1 and u_2 respectively. We observe that the experimental order of convergence is $O(h+k)$ as expected from what has been lectured. Above we found the CFL condition $|r| \leq 1$, this was rigorously upheld during testing.

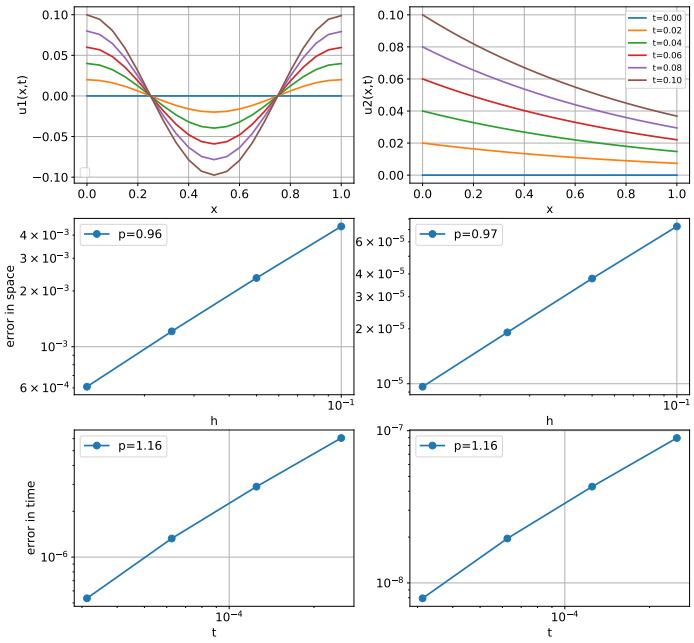

Figure 5: Figure showing how the upwind scheme performed for u_1 and u_2.

The Lax-Wendroff scheme

The derivation of the Lax-Wendroff scheme is somewhat more complicated when a is dependent on x. We derive the scheme from the equations

$$u_t = f - au_x$$
$$u_{tt} = f_t - af_x + a^2u_{xx} + aa_xu_x.$$

Substituting these in the Taylor expansion of $u(x, t+k)$ gives

$$u(x,t+k) = u + ku_t + \frac{1}{2}k^2u_{tt} + O(k^3) = u + k\left(f - au_x\right) + \frac{1}{2}k^2\left(f_t - af_x + a^2u_{xx} + aa_xu_x\right) + O(k^3)$$
$$= u + ka\left(\frac{1}{2}ka_x - 1\right)u_x + \frac{1}{2}k^2a^2u_{xx} + kf + \frac{1}{2}k^2f_t - \frac{1}{2}k^2af_x + O(k^3).$$

We now discretize with central differences in space, and arrive at

$$U_m^{n+1} = \left(1 - r_m^2\right)U_m^n + \left(\frac{1}{2}r_m^2 + \frac{1}{2}r_m - \frac{1}{4}hr_m(r_x)_m\right)U_{m-1}^n + \left(\frac{1}{2}r_m^2 - \frac{1}{2}r_m + \frac{1}{4}hr_m(r_x)_m\right)$$
$$+ k(f)_m^n + \frac{1}{2}k^2(f_t)_m^n - \frac{1}{2}k^2a_m(f_x)_m^n.$$

For this problem we chose exactly the same test functions as for the upwind scheme. Figure 4 shows the numerical solution and log-log plots of the error in both space and time for u_1 and u_2 respectively. Notice the constant extension from the interior to the out-flow boundary. We suspect that this was a big source of error, since its a low order approximation, and could explain the low order of the method. From what was lectured, we would expect order of convergence $O(h^2 + k^2)$, but only order one in time and order one in space was observed for most problems. u_1 was able to provide second order in space, a possible explanation for this could be the CLF-condition. A preliminary look at the monotonicity of our scheme show that the x dependence of the scheme complicates the CFL-condition. Our testing was based on the CFL-condition from the lecures. In the lectures we learned that expanding derivatives before discrediting is generally a bad idea. This could be another explanation for the low order, but further theoretical investigation would be required. In general there seems to be some theoretical issues with the scheme.

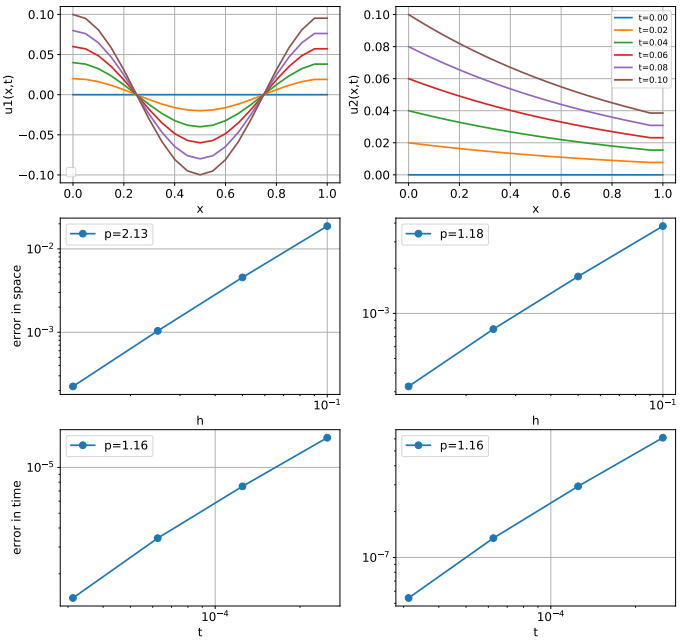

Figure 6: Figure showing how the Lax-Wendroff scheme performed for u_1 and u_2.

4 Conclusion

In this project we implemented schemes with different irregularities for heat distribution in anisotropic materials. Theoretical results agreed with our numerical test. In the second part of the

project where we looked at a transport equation. We proved results for the upwind scheme and they were confirmed in our numerical test. There were some problems with the Lax-Wendroff scheme, and $O(h^2 + k)$ was the best order we were able to obtain.